

# Atomic Josephson junction with two bosonic species

Giovanni Mazzarella<sup>1</sup>, Marco Moratti<sup>1</sup>, Luca Salasnich<sup>2</sup>, Mario Salerno<sup>3</sup>, and Flavio Toigo<sup>1</sup>

<sup>1</sup>Dipartimento di Fisica "Galileo Galilei" and CNISM, Università di Padova, Via Marzolo 8, 35131 Padova, Italy

<sup>2</sup>CNR-INFM and CNISM, Università di Padova, Via Marzolo 8, 35131 Padova, Italy

<sup>3</sup>Dipartimento di Fisica "E.R. Caianiello" and CNISM, Università di Salerno, Via Allende 1, 84081 Baronissi (SA), Italy

**Abstract.** We study an atomic Josephson junction (AJJ) in presence of two interacting Bose-Einstein condensates (BECs) confined in a double well trap. We assume that bosons of different species interact with each other. The macroscopic wave functions of the two components obey to a system of two 3D coupled Gross-Pitaevskii equations (GPE). We write the Lagrangian of the system, and from this we derive a system of coupled ordinary differential equations (ODE), for which the coupled pendula represent the mechanic analogous. These differential equations control the dynamical behavior of the fractional imbalance and of the relative phase of each bosonic component. We perform the stability analysis around the points which preserve the symmetry and get an analytical formula for the oscillation frequency around the stable points. Such a formula could be used as an indirect measure of the inter-species s-wave scattering length. We also study the oscillations of each fractional imbalance around zero and non zero – the macroscopic quantum self-trapping (MQST) – time averaged values. For different values of the inter-species interaction amplitude, we carry out this study both by directly solving the two GPE and by solving the corresponding coupled pendula equations. We show that, under certain conditions, the predictions of these two approaches are in good agreement. Moreover, we calculate the crossover value of the inter-species interaction amplitude which signs the onset of MQST.

PACS numbers: 03.75.Lm, 03.75.Mn, 03.75.Kk

Submitted to: J. Phys. B: At. Mol. Phys.

## 1. Introduction

The prediction [1] of Bose-Einstein condensation and the realization in the laboratory of BECs [2] paved the way to a lot of important theoretical and experimental developments. One of these is the study of the atomic counterpart [3, 4, 5, 6] of the Josephson effect which occurs in superconductor-oxide-superconductor junctions [7]. In [3, 4, 5, 6], realization of AJJ are taken into account from a theoretical point of view. Few years ago, Albiez et al. [8] provided an experimental realization of the AJJ. In 2007 Gati et al. [9] reviewed the experimental realization of the AJJ focusing on the data obtained experimentally with the predictions of a many-body two-mode model [10] and a mean-field description. Under certain conditions, a coherent transfer of matter consisting of condensate bosons flows across the junction. In the above references the AJJ physics is explored in presence of a single bosonic species. The possibility to manage via magnetic and optical Feshbach resonances the intra- and inter-species interactions [11, 12] makes BEC mixtures very promising candidates to successfully investigate quantum coherence and nonlinear phenomena such as the existence of self-trapped modes and intrinsically localized states. Localized states induced by the nonlinearity were shown to be quite generic for multicomponent systems in external trapping potentials. In particular, the emergence of coupled bright solitons from the modulational instability of binary mixtures of BECs in optical lattices was found numerically in [13]. More sophisticated coupled localized states of two-component condensates both in optical lattices and in parabolic traps were reported in [14]. The existence of dark-bright states of binary BEC mixtures was demonstrated in [15]. On the other hand, the existence of localized states of different symmetry type (mixed symmetry states) was numerically and analytically demonstrated in [16]. Properties of coupled gap solitons in binary BEC mixtures with repulsive interactions were also analyzed in the multidimensional case [17] as well as for combined linear and nonlinear optical lattices [18]. Although gap-soliton breathers of multicomponent GPE involving periodic oscillations of the two components densities localized on adjacent sites of an optical lattice have been found [16] (in analogy to what was done for single component case in [6], such states can also be seen as matter wave realizations of Josephson junctions), no much numerical and theoretical study has been done until now on AJJ of binary mixtures.

Recently, this has been considered in [19, 20] for the case of a bosonic binary mixtures trapped in a double well potential, for which a coupled pendula system of ODE for the temporal evolution of the relative population and relative phase of each component, was derived. Using this reduced system, the authors of [20] have predicted the analogous of the macroscopic quantum self-trapping phenomenon for a single bosonic component [4]. No comparison between the reduced ODE system and the full GPE dynamics has been performed, so that the question of the validity of such prediction remains open. For single component condensates, Salasnich et al. [5] have shown that a good agreement exists between the results obtained from the GPE and those of the ODE. Similar agreement was obtained in [6] for AJJ realized with weakly interacting

solitons localized in two adjacent wells of an optical lattice. However, the situation may be quite different for multicomponent condensates, due to the interplay of intra- and inter-species interactions which enlarge the number of achievable states (for instance, mixed symmetry states can exist only in presence of the inter-species interaction) as well as their stability, making the system much more complicated.

The aim of the present paper is just to perform a systematic investigation of possible Josephson oscillations which can arise in binary BEC mixtures trapped in a double well potential, as a function of the system parameters. To this regard, we derive the reduced coupled pendula system proceeding from a Lagrangian formulation and from the canonical equations of motion. We show that for certain conditions and range of parameters there exists a good agreement between the solutions of the two GPE and the predictions provided by the coupled pendula equations. We look for the stationary points that preserve the symmetry and study their stability; we get an analytical formula for the oscillation frequencies around the equilibrium points. This formula shows the possibility to determine the inter-species s-wave scattering length from the frequency.

We analyze the influence of the inter-species interaction on the temporal evolution of each relative population. In particular, by employing the coupled pendula equations we show the existence of MQST when the inter-species interaction amplitude is greater than a certain value, for which we are able to provide an analytical formula. As done by Satija et al. [20], we calculate the values of the relative populations associated to the degenerate GPE states that break the symmetry of the fractional imbalances. In addition, we perform the stability analysis by explicitly calculating the associated oscillation frequencies. We, moreover, show that the MQST-like evolution obtained by solving the coupled pendula equations is close to that one obtained by integrating the two coupled GPE.

Proceeding from the works of Albiez et al. [8] and of Gati et al. [9], we correlate our theoretical work with experiments. Finally, we draw our conclusions.

## 2. A JJ with two bosonic species: quasi-analytical approach

We consider two Bose-Einstein condensates of repulsively interacting Bosons with different atomic species denoted below by 1 and 2. We suppose that the two BECs are confined in a double-well trap produced, for example, by a far off-resonance laser barrier that separates each trapped condensate in two parts, L (left) and R (right). We assume, moreover, that the two condensates interact with each other. In the mean field approximation, the macroscopic wave functions  $\psi_i(\mathbf{r};t)$ , ( $i = 1,2$ ), of the interacting Bose-Einstein condensates in a trapping potential  $V_{\text{trap}}(\mathbf{r})$  at zero-temperature satisfy the two coupled Gross-Pitaevskii equations

$$i\hbar \frac{\partial \psi_i}{\partial t} = -\frac{\hbar^2}{2m_i} \nabla^2 \psi_i + [V_{\text{trap}}(\mathbf{r}) + g_{ii} |\psi_i|^2 + g_{ij} |\psi_j|^2] \psi_i \quad (1)$$

Here  $\nabla^2$  denotes the 3D Laplacian, and  $\psi_i(\mathbf{r}; t)$  is subject to the normalization condition

$$\int d\mathbf{x} d\mathbf{y} dz |\psi_i(\mathbf{x}; \mathbf{y}; z)|^2 = N_i; \quad (2)$$

with  $N_i$  the number of bosons of the  $i$ th species. Similarly,  $m_i$ ,  $a_i$  and  $g_i = 4\pi\hbar^2 a_i/m_i$  denotes the atomic mass, the  $s$ -wave scattering length and the intra-species coupling constant of the  $i$ th species;  $g_{ij} = 2\pi\hbar^2 a_{ij}/m_r$  ( $i \neq j$ ) is the inter-species coupling constant, with  $m_r = m_i m_j / (m_i + m_j)$  the reduced mass, and  $a_{ij}$  the associated  $s$ -wave scattering length. In the following, we shall consider both  $g_i$  and  $g_{ij}$  as free parameters,

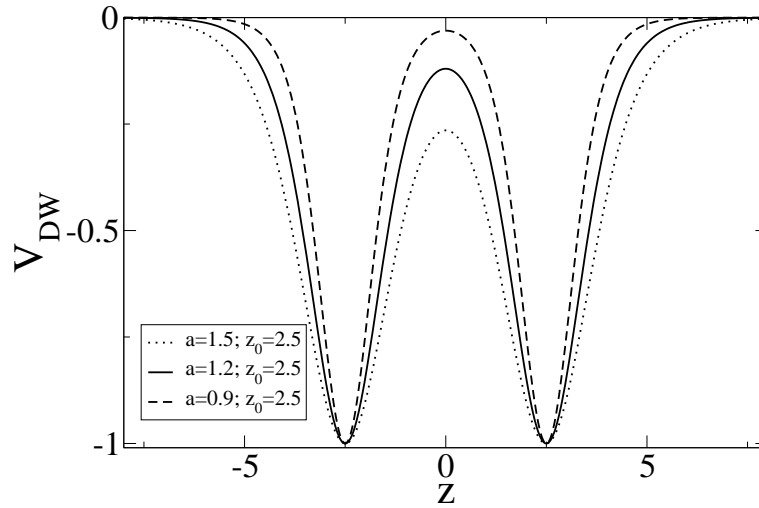


Figure 1. The double well potential (4) as a function of  $z$ . Lengths are measured in units of  $a_{z,1} = a_{z,2} = a_z$ , and energies in units of  $\hbar^2/m_i = \hbar^2/m_j = \hbar^2/m_r$ .

due to the possibility to change the scattering lengths  $a_i$  and  $a_{ij}$  at will by using the technique of Feshbach resonances. Here we take into account the case in which the two BECs interact attractively, see [11] and [21].

The trapping potential for both components is taken to be the superposition of a strong harmonic confinement in the radial ( $x$ - $y$ ) plane and of a double well (DW) potential in the axial ( $z$ ) direction. For the  $i$ th component, we model this trapping potential in the form

$$V_{\text{trap}}(\mathbf{r}) = \frac{m_i \hbar^2}{2} (x^2 + y^2) + V_{\text{DW}}(z); \quad (3)$$

where, for symmetric configurations in the  $z$  direction, we model the DW potential as

$$\begin{aligned} V_{\text{DW}}(z) &= V_L(z) + V_R(z); \quad V_L(z) = \frac{\hbar^2}{V_0} \text{sech}^2\left(\frac{z+z_0}{a}\right); \\ V_R(z) &= \frac{\hbar^2}{V_0} \text{sech}^2\left(\frac{z-z_0}{a}\right); \quad V_0 = \hbar^2 \left[1 + \text{sech}^2\left(\frac{2z_0}{a}\right)\right]^{-1}; \end{aligned} \quad (4)$$

ie. the combination of two Pöschl-Teller (PT) potentials,  $V_L(z)$  and  $V_R(z)$ , separated by a potential barrier, the height of which can be changed by varying  $a$ , centered around the points  $-z_0$  and  $z_0$  (see Fig. 1). Note that the usage of PT potentials is only for

the benefit of improving accuracy in our numerical GPE calculations (see below), taking advantage of the integrability of the underlying linear system. We remark, however, that the obtained results are of generic validity also for more confining (e.g. not saturating to zero at large distances) double well potentials.

We are interested to study the dynamical oscillations of the populations of each condensate between the left (L) and right (R) wells when the barrier is large enough so that the link is weak. To exploit the strong harmonic confinement in the (x-y) plane and get the effective 1D equations describing the dynamics in the z direction, we write the Lagrangian associated to the GPE equations in (1)

$$L = \int d^3r \sum_{i=1,2} \left[ \frac{\hbar^2}{2m_i} \left( i\vec{\nabla} \cdot \frac{\partial}{\partial t} + \frac{\vec{\nabla}^2}{2m_i} \right) \psi_i \right. \\ \left. V_{\text{trap}}(r) |\psi_i|^2 - \frac{g_i}{2} |\psi_i|^4 - g_{ij} |\psi_i|^2 |\psi_j|^2 \right]; \quad (5)$$

where  $\psi_i$  denotes the complex conjugate of  $\psi_i$ , and  $i \neq j$  and adopt the ansatz [22]

$$\psi_i(x; y; z; t) = \frac{1}{a_{z,i}} \exp \left[ -\frac{x^2 + y^2}{2a_{z,i}^2} \right] f_i(z; t); \quad (6)$$

where  $a_{z,i} = \frac{\hbar}{m_i \omega_i}$  and the  $f_i(z; t)$  obey  $\int_{-1}^{R+1} dz |\psi_i(z)|^2 = N_i$ , so that the normalization condition Eq. (2) is satisfied. By inserting this ansatz (6) in (5) and performing the integration in the radial plane, we obtain the effective 1D Lagrangian for the fields  $f_i(z; t)$

$$\tilde{L} = \int dz \sum_{i=1,2} \left[ \frac{\hbar^2}{2m_i} \left( i\frac{\partial}{\partial t} + \frac{\partial^2}{2m_i \partial z^2} \right) f_i \right. \\ \left. (V_i + V_{\text{DW}}(z)) |f_i|^2 - \frac{g_i}{2} |f_i|^4 - g_{ij} |f_i|^2 |f_j|^2 \right]; \quad (7)$$

where the effective parameters for the 1D dynamics are given in terms of the original ones by:  $\tilde{m}_i = \frac{\hbar^2}{2m_i a_{z,i}^2} + \frac{m_i \omega_i^2 a_{z,i}^2}{2}$ ,  $\tilde{g}_i = \frac{g_i}{2 a_{z,i}^2}$ , and  $\tilde{g}_{ij} = \frac{g_{ij}}{(a_{z,i}^2 + a_{z,j}^2)}$ . By varying  $\tilde{L}$  with respect to  $f_i$ , we obtain the 1D GPE for the field  $f_i$

$$i\hbar \frac{\partial f_i}{\partial t} = \frac{\hbar^2}{2m_i} \frac{\partial^2 f_i}{\partial z^2} + [V_i + V_{\text{DW}}(z) + \tilde{g}_i |f_i|^2 + \tilde{g}_{ij} |f_j|^2] f_i; \quad (8)$$

It is possible to study the AJJ dynamics described by Eq. (8) by using the two-mode approximation discussed by Milburn et al. in [10]. In particular, we assume, for each  $f_i$ , the following time-dependent wave function decomposition

$$f_i(z; t) = \frac{1}{N_i} \left[ L_i(t) \phi_L^i(z) + R_i(t) \phi_R^i(z) \right]; \quad (9)$$

where

$$\phi_i(t) = \frac{1}{N_i} e^{i\phi_i(t)}; \quad (10)$$

with  $i = L, R$ , and a constant total number of particles given by  $N_i^L + N_i^R = j_i^L(t)j_i^L + j_i^R(t)j_i^R$ , with  $\int_{-1}^{+1} dz j_i^L(z)j_i^L = 1$  and  $\int_{-1}^{+1} dz j_i^L(z)j_i^R(z) = 0$ . Neglecting terms of order greater than two in the overlaps of the  $\psi$ 's, we can write the Lagrangian (7) in terms of  $N_i^L$  and  $N_i^R$  as

$$\begin{aligned} L = & \sum_{i=1,2} \left[ \frac{\hbar^2}{2m_i} \dot{N}_i^L \dot{N}_i^L + \frac{\hbar^2}{2m_i} \dot{N}_i^R \dot{N}_i^R - E_i^L N_i^L - E_i^R N_i^R \right. \\ & + 2K_i N_i^L N_i^R \cos(\phi_i^L - \phi_i^R) + \frac{U_i^L}{2} (N_i^L)^2 + \frac{U_i^R}{2} (N_i^R)^2 \Big] \\ & + U_{12} N_1^L N_2^L + U_{12} N_1^R N_2^R ; \end{aligned} \quad (11)$$

where

$$\begin{aligned} E_i &= \int_{-1}^1 dz \left[ \frac{\hbar^2}{2m_i} \left( \frac{d\psi_i}{dz} \right)^2 + (V_{DW} + \frac{\hbar^2}{2m_i a_i^2} + \frac{m_i!^2 a_i^2}{2}) (\psi_i)^2 \right] ; \\ U_i &= g_i \int_{-1}^1 dz (\psi_i)^4 ; \quad U_{12} = g_{12} \int_{-1}^1 dz (\psi_1)^2 (\psi_2)^2 ; \\ K_i &= \int_{-1}^1 dz \left[ \frac{\hbar^2}{2m_i} \frac{d\psi_i^L}{dz} \frac{d\psi_i^R}{dz} + V_{DW} \psi_i^L \psi_i^R \right] ; \end{aligned} \quad (12)$$

One may get a good approximation for the functions  $\psi_i^L(z)$  and  $\psi_i^R(z)$  when the double well potential  $V_{DW}(z)$  is such that the two lowest energy eigenvalues of the corresponding Schrodinger equation constitute a closely spaced doublet well separated from the higher excited levels, and the  $g$ 's are not too large (see, for example, [10]). If the real symmetric function  $\psi_i^S(z)$  and the real antisymmetric function  $\psi_i^A(z)$  are the wave functions of the ground state and of the first excited state, respectively, then  $\psi_i^L(z)$  and  $\psi_i^R(z)$  may be chosen as

$$\psi_i^L(z) = \frac{\psi_i^S(z) + \psi_i^A(z)}{\sqrt{2}} ; \quad \psi_i^R(z) = \frac{\psi_i^S(z) - \psi_i^A(z)}{\sqrt{2}} ; \quad (13)$$

Remember that  $\psi_i^S(z)$  and  $\psi_i^A(z)$  satisfy the relations:  $\int_{-1}^{+1} dz j_i^S(z)j_i^S = \int_{-1}^{+1} dz j_i^A(z)j_i^A = 1$  and  $\int_{-1}^{+1} dz \psi_i^A(z)\psi_i^S(z) = 0$ . Having chosen  $V_{DW}(z)$  as the sum of two of two Pöschl-Teller (PT) wells (see Eq. (4)), the functions  $\psi_i^L(z)$  and  $\psi_i^R(z)$  may be analytically calculated following a perturbative approach. Let us consider the eigenvalues problem corresponding to Eq. (8) with  $g_i = g_{ij} = 0$ . We know exactly the wave functions for this eigenvalues problem when the potential is given by a single  $V(z)$  ( $i = L, R$ ), for example  $V_L(z)$ . The wave function of the ground state is [23]

$$\begin{aligned} \psi_i^{(L,PT)}(z) &= A \left[ 1 - \tanh^2 \left( \frac{z + z_0}{a} \right) \right]^{B_i/2} \\ B_i &= \frac{1}{2} + \frac{1}{\frac{\hbar^2}{2m_i V_0 a^2} + \frac{1}{4}} ; \end{aligned} \quad (14)$$

In Eq. (14)  $A$ , equal for both sides, ensures the normalization of the wave function. Since we are assuming that the two lowest energetic levels are well separated from the

higher ones, when the potential is perturbed by the presence of  $V_R(z)$ , we look for the eigenstates in the form of a linear superposition of  $\psi_i^{(L,P,T)}$  and  $\psi_i^{(R,P,T)}$ . For each component, to the first order of such a perturbative theory, the ground state wave function  $\psi_i^S(z)$  and the first excited state wave function  $\psi_i^A(z)$  read

$$\begin{aligned}\psi_i^S(z) &= M_S (\psi_i^{(L,P,T)}(z) + \psi_i^{(R,P,T)}(z)) \\ \psi_i^A(z) &= M_A (\psi_i^{(L,P,T)}(z) - \psi_i^{(R,P,T)}(z)) : \end{aligned} \quad (15)$$

Here  $M_S$  and  $M_A$  ensure the normalization of  $\psi_i^S(z)$  and  $\psi_i^A(z)$ , respectively. Note that  $K_i$  is equal to  $(E_i^A - E_i^S)/2$ , with  $E_i^S$  and  $E_i^A$ , also perturbatively calculated, the energies associated to  $\psi_i^S(z)$  and  $\psi_i^A(z)$ , respectively. The quantity

$$\Omega_i = \frac{(E_i^A - E_i^S)}{2\hbar} \quad (16)$$

is the Rabi frequency. This frequency characterizes the oscillations of a particle between the states  $\psi_i^L$  and  $\psi_i^R$ . By using Eq. (15) in the decomposition (13), we are able to write the functions  $\psi_i^L(z)$  and  $\psi_i^R(z)$  in terms of  $\psi_i^{(L,P,T)}(z)$  and  $\psi_i^{(R,P,T)}(z)$  in the following way

$$\begin{aligned}\psi_i^L &= \frac{(M_S + M_A) \psi_i^{(L,P,T)} + (M_S - M_A) \psi_i^{(R,P,T)}}{2\hbar} \\ \psi_i^R &= \frac{(M_S - M_A) \psi_i^{(L,P,T)} + (M_S + M_A) \psi_i^{(R,P,T)}}{2\hbar} : \end{aligned} \quad (17)$$

Note that  $\psi_i^S(z)$  and  $\psi_i^A(z)$ , and the associated energies, may be numerically found as the wave functions of the two lowest states of the eigenvalues problem corresponding to Eq. (8) in absence of interactions. Then, by using the decomposition (13), one calculates the functions  $\psi_i^L(z)$  and  $\psi_i^R(z)$ . We have verified that the perturbative theory provides practically the same results as the numerical approach.

Let us, now, focus on the Lagrangian (11). The conjugate moments of the generalized coordinates  $N_i$  and  $\phi_i$  are given by

$$p_{N_i} = \frac{\partial L}{\partial N_i} = 0 ; \quad p_{\phi_i} = \frac{1}{\hbar} \frac{\partial L}{\partial \phi_i} = N_i : \quad (18)$$

The Hamiltonian of the system is

$$\begin{aligned}H &= \sum_{i=1,2} [p_i^L E_i^L + p_i^R E_i^R] - \sum_{i=1,2} 2K_i p_i^L p_i^R \cos(\phi_i^L - \phi_i^R) + \\ &+ \sum_{i=1,2} \left[ \frac{U_i^L}{2} p_i^L{}^2 + \frac{U_i^R}{2} p_i^R{}^2 \right] + U_{12}^L p_1^L p_2^L + U_{12}^R p_1^R p_2^R : \end{aligned} \quad (19)$$

The evolution equations for the fractional imbalance  $z_i = (N_i^L - N_i^R)/N_i$  and for the relative phase  $\phi_i = \phi_i^R - \phi_i^L$  for each component are derived from the canonical equations

associated to the Hamiltonian (19)

$$\underline{p}_i = \frac{1}{\hbar} \frac{\partial H}{\partial \dot{z}_i} ; \quad \underline{\tau}_i = \frac{1}{\hbar} \frac{\partial H}{\partial \dot{p}_i} ; \quad (20)$$

By subtracting the equation for  $\underline{p}_i^L$  from the one for  $\underline{p}_i^R$ , we obtain the equation for the temporal evolution of  $z_i$ . Similar arguments leads to the equation for  $\dot{z}_i(t)$ . In the following, we shall assume two wells to be symmetric, i.e.  $E_i^L = E_i^R$ ,  $U_i^L = U_i^R = U_i$ ,  $U_{12}^L = U_{12}^R = U_{12}$ . The fractional imbalance and the relative phase for each component vary in time according to the following (coupled pendula) equations:

$$\ddot{z}_i = -\frac{2}{\hbar^2} K_i \sin \left[ \frac{1}{2} \left( \frac{2\pi}{\tau_i} \right) z_i \right] \cos \left[ \frac{1}{2} \left( \frac{2\pi}{\tau_i} \right) z_i \right] + \frac{U_i N_i z_i}{\hbar^2} + \frac{2K_i z_i}{\hbar^2} \cos \left[ \frac{1}{2} \left( \frac{2\pi}{\tau_i} \right) z_i \right] + \frac{U_{12} N_j z_j}{\hbar^2} ; \quad (21)$$

Note that when  $U_{12} = 0$ , equations (21) reduce to the usual equations for a single component obtained in [4]. At this point, we observe that it is possible to obtain Eq. (21) proceeding from the following equations

$$N_i \ddot{z}_i = -\frac{1}{\hbar^2} \frac{\partial \tilde{H}}{\partial z_i} ; \quad N_i \dot{\tau}_i = \frac{1}{\hbar^2} \frac{\partial \tilde{H}}{\partial \dot{z}_i} ; \quad (22)$$

where  $\tilde{H}$  is

$$\tilde{H} = \sum_{i=1,2} \left[ \frac{2K_i N_i}{\hbar^2} \left( \frac{1}{2} \left( \frac{2\pi}{\tau_i} \right) z_i \right) \cos \left[ \frac{1}{2} \left( \frac{2\pi}{\tau_i} \right) z_i \right] + \frac{U_i}{2} N_i z_i^2 + U_{12} N_1 N_2 z_1 z_2 \right] ; \quad (23)$$

To x ideas, let us consider, as done in [12], a mixture of two bosonic isotopes of the same atom, so that one may have different intra-species and inter-species interactions. For simplicity, for the time being we will neglect the mass difference between the two species. We compare the temporal behavior of the fractional imbalances obtained integrating Eq. (8) with the  $z_i(t)$  obtained by solving the coupled differential equations (21). To this end, in the wave functions (14) we assume that the quantities  $B_i$  are the same for both species, and in the double well potential (4) we set  $a = 1.2$  and  $z_0 = 2.5$ , as illustrated by the continuous line of Fig. 1. We calculate the parameters  $U_i$ ,  $U_{12}$ , and  $K_1 = K_2 = K$  by using Eqs. (12). Note that the value of  $K$  (equal, for the above values of  $a$  and  $z_0$ , to 0.0148), provided by the last formula of Eqs. (12) coincides with  $\frac{\hbar^2}{m_0 \tau_0^2}$ . Here  $\tau_0$  is the oscillation period of  $z_i(t)$  obtained by numerically solving the 1D GPE (8) when  $U_i = U_{12} = 0$ . This period is just equal to  $2\pi/\omega$  with  $\omega$  given by Eq. (16). In Fig. 2, the first panel of each  $z_i(t)$  graph shows the perfect agreement between the two coupled 1D GPE and the coupled pendula equations when the bosons do not interact at all. In the second panel of each  $z_i(t)$  of Fig. 2,  $U_i$  is finite and  $U_{12} = 0$ . Finally, in the last panel,  $U_i$  and  $U_{12}$  are both finite. From the second and the third panels of Fig. 2, we see that the solutions of the ODE system (21) with  $K = 0.0148$  (dot-dashed lines) shows a certain displacement with respect to the ones (dashed lines) predicted by solving the two 1D GPE (8). The continuous lines, in the second and in the third panels of Fig. 2,



represent the solutions of the ODE system (21) with  $K$  obtained via a fitting procedure. The best-fit  $K$ 's that we found are equal to 0.0155 and 0.0151 when only  $U_i \neq 0$  and when  $U_i$  and  $U_{12}$  are both finite, respectively. Notice that these values are very close to the above theoretical estimate of  $K$ , so the coupled pendula equations may be used to consistently describe the AJJ physics.

To gain physical insight in the behavior of the system, we carry out the stability analysis. We study the oscillations around the points for which the time derivatives of  $z_i$  and of  $\dot{\phi}_i$  are zero, i.e. around the stationary points. We diagonalize the Jacobian matrix associated to Eqs. (21). The eigenvalues allow us to determine the frequencies of oscillation around the points of equilibrium. If the  $\omega$ 's are of the form  $i\omega$  (with  $\omega$  a pure real number),  $\omega$  will be the oscillation frequency around stable equilibrium points. By performing the above analysis, we obtain the following classes of stationary points:

- (i)  $z_1 = 0; z_2 = 0; \dot{\phi}_1 = 0; \dot{\phi}_2 = 0$
- (ii)  $z_1 = 0; z_2 = 0; \dot{\phi}_1 = 0; \dot{\phi}_2 = \dots$
- (iii)  $z_1 = 0; z_2 = 0; \dot{\phi}_1 = \dots; \dot{\phi}_2 = 0$
- (iv)  $z_1 = 0; z_2 = 0; \dot{\phi}_1 = \dots; \dot{\phi}_2 = \dots$ ,  
 $z_1 = 0; z_2 = 0; \dot{\phi}_1 = \dots; \dot{\phi}_2 = \dots$ .

We observe that the points of a given class are characterized by the same  $\dots$ . The stationary solution (i) represents a stable equilibrium if  $U_{12}$  satisfies the condition

$$\omega^{(1)} = \frac{\sqrt{\frac{2K_1 + N_1 U_1}{N_1 N_2} (2K_2 + N_2 U_2)}}{p} < U_{12} < \frac{\sqrt{(2K_1 + N_1 U_1) (2K_2 + N_2 U_2)}}{p} \quad (24)$$

provided

$$U_i > \frac{2K_i}{N_i} : \quad (25)$$

The small amplitude oscillations frequency, say  $\omega^{(1)}$ , around the point (i) is

$$\begin{aligned} \omega^{(1)} &= \frac{1}{\hbar} \left( K_1 (2K_1 + U_1 N_1) + K_2 (2K_2 + U_2 N_2) \right)^{1/2} ; \\ &= \frac{4K_1 K_2 (4K_1 K_2 + 2K_1 U_2 N_2 + 2K_2 U_1 N_1 - U_{12}^2 N_1 N_2}{\left( U_1 U_2 N_1 N_2 + (K_1 (2K_1 + U_1 N_1) + K_2 (2K_2 + U_2 N_2))^2 \right)^{1/2}} \end{aligned} \quad (26)$$

with  $+$  and  $-$  corresponding to the normal modes of the linearized system associated to Eq. (21). When  $z_1(0) = z_2(0) = 1$ ,  $U_1 = U_2$ ,  $K_1 = K_2$ , and  $N_1 = N_2$ , the fractional imbalances  $z_i$  oscillate around the point (i) according to the law

$$z_i(t) = z_i(0) \cos \omega^{(1)} t : \quad (27)$$

Let us operate in Eqs. (24), (25), and (26) the replacement  $U_i \rightarrow U_i$ . Then, we obtain the stability conditions and the oscillation frequency associated to the class (iv).

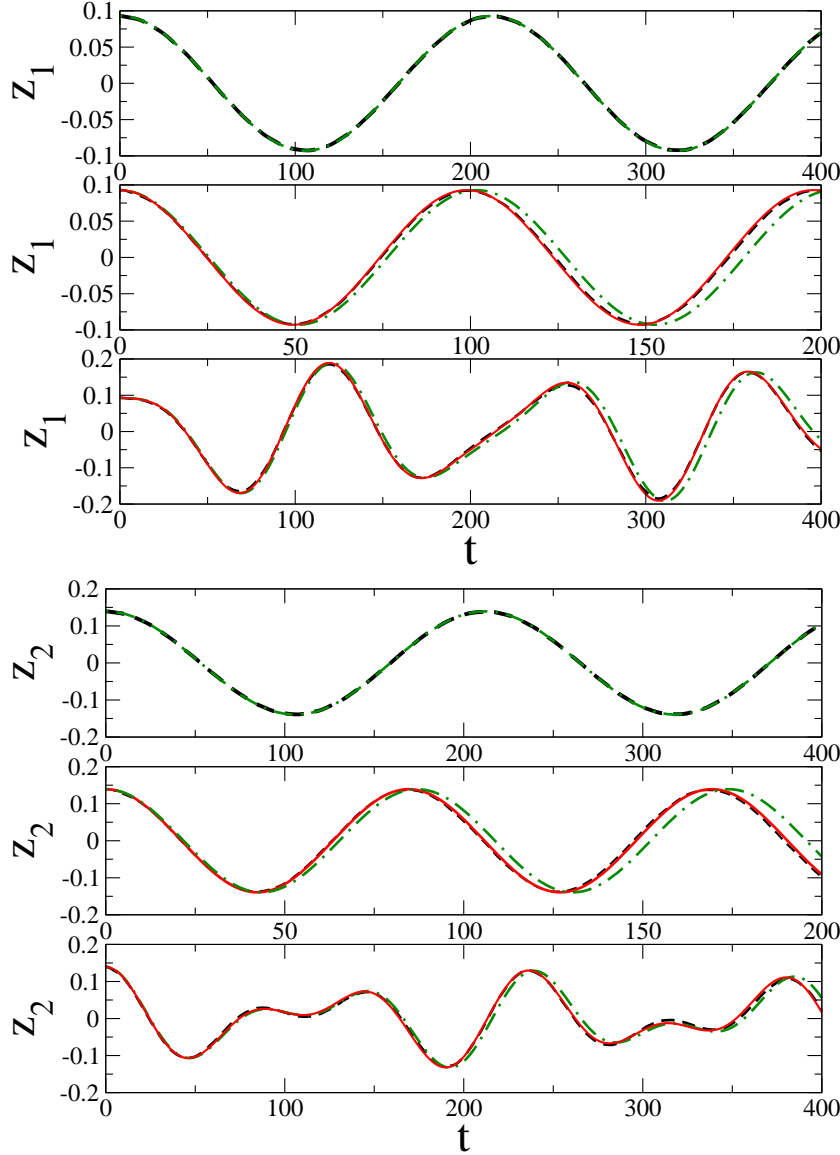


Figure 2. Fractional imbalance of the two bosonic species vs. time. Here  $N_1 = 100$  and  $N_2 = 150$ . In each plot of  $z_i(t)$ , from top to bottom:  $U_1 = U_2 = U_{12} = 0$ ;  $U_1 = U_2 = 0.001; U_{12} = 0$ ;  $U_1 = U_2 = U = 0.001; U_{12} = U = 2$ . The dashed line represents data from integration of Eq. (8), the dot-dashed line represents solution of Eq. (21) with  $K_1 = K_2 = K = 0.0148$ , and the continuous line, in the second and third panels, represents solution of Eq. (21) with the best-fit  $K$ 's, say  $K_{bf}$ . For each  $z_i(t)$ ,  $K_{bf} = 0.0155$  ( $U_1 = U_2 = 0.001; U_{12} = 0$ ) and  $K_{bf} = 0.0151$  ( $U_1 = U_2 = U = 0.001; U_{12} = U = 2$ ). We used the initial conditions  $z_1(0) = 0.1$ ,  $z_2(0) = 0.15$ , and  $\dot{z}_i(0) = 0$ . Time is measured in units of  $(\hbar J)^{-1} = (\hbar J_2)^{-1} = \hbar^{-1}$ , lengths are measured in units of  $a_{\perp,1} = a_{\perp,2} = a_{\perp}$ , and energies in units of  $\hbar J$ .

We have verified that for the stationary points of type (ii), under certain conditions (analytically achievable but very complicated), the eigenvalues of Jacobian matrix are all of the form  $i\omega$ . The small amplitude oscillations frequency, say  $\omega^{(2)}$ , around the point

(ii) is

$$\begin{aligned} \omega_A^{(2)} &= \frac{1}{\hbar} (K_1 (2K_1 + U_1 N_1) + K_2 (2K_2 + U_2 N_2))^{1/2} ; \\ &= \frac{4K_1 K_2 (4K_1 K_2 + 2K_1 U_2 N_2 + 2K_2 U_1 N_1 + U_{12}^2 N_1 N_2 + U_1 U_2 N_1 N_2) + (K_1 (2K_1 + U_1 N_1) + K_2 (2K_2 + U_2 N_2))^2}{4K_1 K_2}^{1/2} : \end{aligned} \quad (28)$$

For the oscillations of  $z_i$  around the point (ii), one may use arguments analogous to the ones employed for the class (i). If we start, now, from the points of the class (ii), and replace  $U_i$  with  $-U_i$ , we get the stability regions and the oscillation frequency for the point of type (iii). Let us focus, to  $x$  the ideas, on the frequency (26), and on the formula of Eq. (12) which gives the inter-species interaction amplitude  $U_{12}$ . We note that  $g_{12}$  is directly related to the inter-species s-wave scattering length. This quantity, then, can be determined from the oscillation frequency (26) once one keeps fixed  $K_i, U_i$ , and  $N_i$ . We will discuss this point with more details in the following.

At this point, it is worth observing that, because of the non linearity associated to the inter- and intra-species interactions, there is a class of degenerate GPE eigenstates that breaks the  $z_i$  symmetry. Let assume that  $U_1 = U_2 = U$ ,  $K_1 = K_2 = K$ , and  $N_1 = N_2 = N$ . In correspondence of  $z_i = 0$ , we have looked for non zero stationary solutions of the system (21). We have found four classes of fractional imbalances corresponding to the  $z_i$  broken symmetry; we have verified that two of these classes do not correspond to a stable equilibrium. Let us consider the two classes describing stable equilibrium, say I and II. For the class I, we have

$$\begin{aligned} z_{1, \text{sb}}^{(I)} &= \frac{1}{N} \frac{2K}{(U + U_{12})^2} \\ z_{2, \text{sb}}^{(I)} &= z_{1, \text{sb}}^{(I)} ; \end{aligned} \quad (29)$$

provided  $j(U + U_{12})j > 2K = N$ . When  $0 < U < 2K = N$ , the solution (29) is always stable, and the corresponding oscillation frequency is

$$\omega_A^{(I)} = \frac{1}{\hbar} \frac{2K}{N (U + U_{12})^2} \quad 4K^2 : \quad (30)$$

For  $U > 2K = N$ , the solution (29) is stable when

$$\begin{aligned} U_{12} &> U_{12}^{(I)} = \frac{2K}{N} \quad UN = 2K \\ &+ \frac{3^{1/3} (9UN = 2K + \sqrt{3 + 81(UN = 2K)^2})^{2/3}}{3^{2/3} (9UN = 2K + \sqrt{3 + 81(UN = 2K)^2})^{1/3}} : \end{aligned} \quad (31)$$

The corresponding oscillation frequency is

$$\omega_B^{(I)} = \frac{1}{\hbar} \frac{2K}{N (U + U_{12})^2} + 4K^2 \frac{U_{12}}{U + U_{12}} : \quad (32)$$

It is possible determine the crossover value, say  $U_{12}^{(\text{I,cr})}$ , of the inter-species interaction strength signing the onset of the self-trapping. We start evaluating the

Hamiltonian (23) in  $z_i = z_{i, \text{sb}}^{(\text{I})}$  and  $\phi_i = 0$ . Let us denote the energy obtained in this way by  $E^{(\text{I})}$ . This energy reads

$$E^{(\text{I})} = \frac{4K^2}{U + U_{12}} + N^2 (U + U_{12}) : \quad (33)$$

Then, we evaluate the Hamiltonian (23) at  $t = 0$ , i.e.  $H(z_i(0); \phi_i(0))$ . We require that

$$H(z_i(0); \phi_i(0)) > 4KN \quad (34)$$

with  $4KN$  the value got by  $E^{(\text{I})}$  when  $z_{i, \text{sb}}^{(\text{I})} = 0$ , i.e. when  $2K = N(U + U_{12})$ . Then, we get

$$U_{12}^{(\text{I}, \text{cr})} = \frac{K}{N} \frac{h}{z_1(0)z_2(0)} \frac{UN}{2K} \sum_{i=1,2} z_i(0)^2 + 2 \sum_{i=1,2} \frac{1}{z_i(0)^2} \cos \phi_i(0) : \quad (35)$$

When the condition  $U_{12} > U_{12}^{(\text{I}, \text{cr})}$  is satisfied, the system will be selftrapped. For the solution of the type II, we have

$$z_{1, \text{sb}}^{(\text{II})} = \frac{1}{N(U + U_{12})} \sqrt{\frac{2K}{U - U_{12}}}^2$$

$$z_{2, \text{sb}}^{(\text{II})} = z_{1, \text{sb}}^{(\text{II})} ; \quad (36)$$

provided that  $j(U - U_{12})j > 2K = N$ . When  $0 < U < 2K = N$ , this solution is always stable and is characterized by the oscillation frequency

$$\omega_A^{(\text{II})} = \frac{1}{\hbar} \sqrt{N(U - U_{12})^2 + 4K^2} : \quad (37)$$

When  $U > 2K = N$ , the solution (36) is stable if

$$U_{12} < U_{12}^{(\text{II})} = \frac{2K}{N} \quad UN = 2K$$

$$\frac{3^{1=3} \left( (UN=2K)^3 + \frac{UN=2K}{3+81(UN=2K)^2} \right)^{2=3}}{3^{2=3} \left( (UN=2K)^3 + \frac{UN=2K}{3+81(UN=2K)^2} \right)^{1=3}} ; \quad (38)$$

and the corresponding oscillation frequency reads

$$\omega_B^{(\text{II})} = \frac{1}{\hbar} \sqrt{N(U - U_{12})^2 + 4K^2} \frac{U + U_{12}}{U_{12} U} : \quad (39)$$

Also for the solution II, it is possible to determine the inter-species interaction amplitude which signs the selftrapping onset, say  $U_{12}^{(\text{II}, \text{cr})}$ , by using the same argument employed for the class I. Also in this case, we proceed by evaluating the Hamiltonian (23) in  $z_i = z_{i, \text{sb}}^{(\text{II})}$  and  $\phi_i = 0$ . Let us denote the energy obtained in this way by  $E^{(\text{II})}$ . This energy reads

$$E^{(\text{II})} = \frac{4K^2}{U - U_{12}} + N^2 (U - U_{12}) : \quad (40)$$

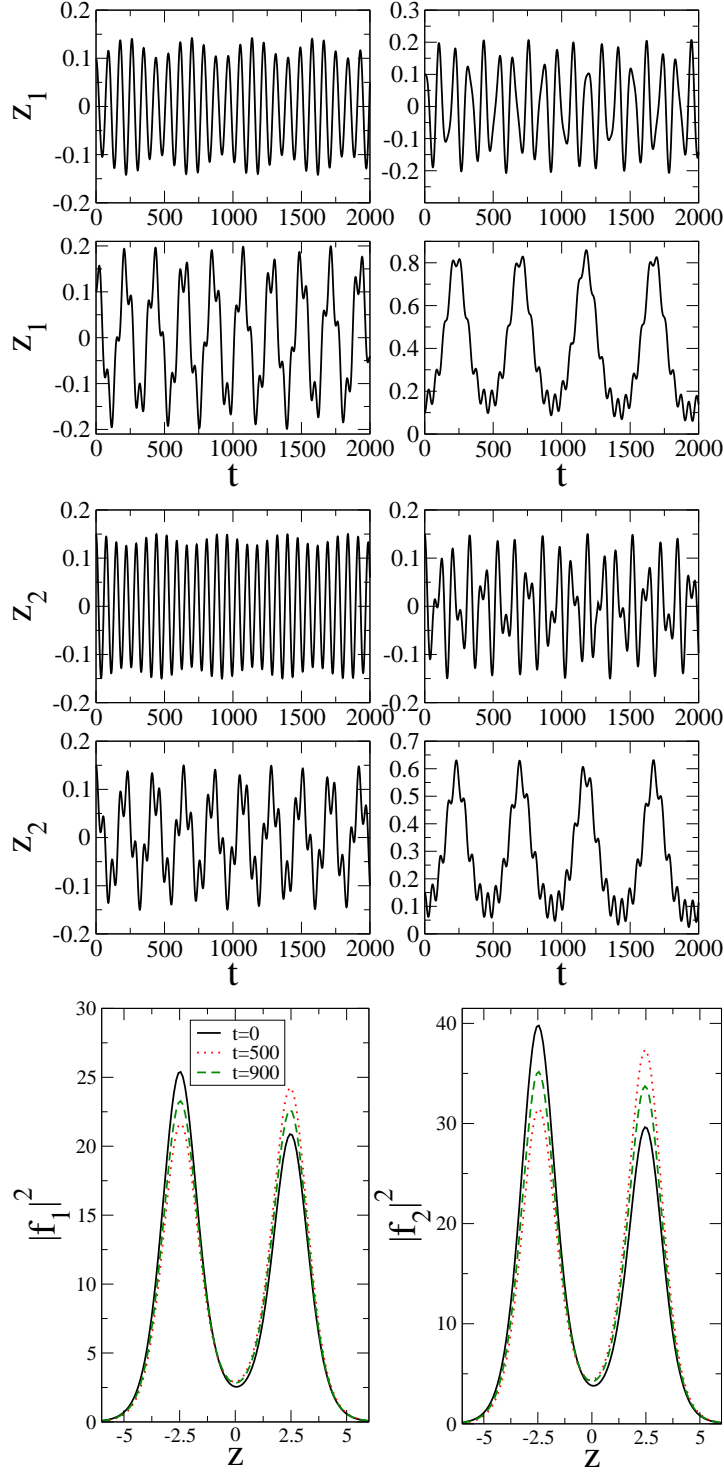


Figure 3. Fractional imbalances of the first and second bosonic species as functions vs. time. Here  $N_1 = 100$  and  $N_2 = 150$ ,  $K_1 = K_2 = 0.0148$ , and  $U_1 = U_2 = U = 0.1K_1$ . Plots are for different values of  $U_{12}$ .  $U_{12} = U$  and  $U_{12} = 1/2 U$  (the two upper panels of each  $z_i(t)$ , from left to right);  $U_{12} = U$  and  $U_{12} = 1/2 U$  (the two lower panels of each  $z_i(t)$ , from left to right). We used the initial conditions  $z_1(0) = 0.1$ ,  $z_2(0) = 0.15$ , and  $\phi_1(0) = 0$ . Here, we report the profiles  $|f_1|^2$  and  $|f_2|^2$  as functions of  $z$  and for different values of time, as displayed in the figure. The quantities  $|f_i|^2$  are obtained by integrating Eq. (8) when  $U_{12} = 1/2 U$ . Units are as in Fig. 1 and Fig. 2.

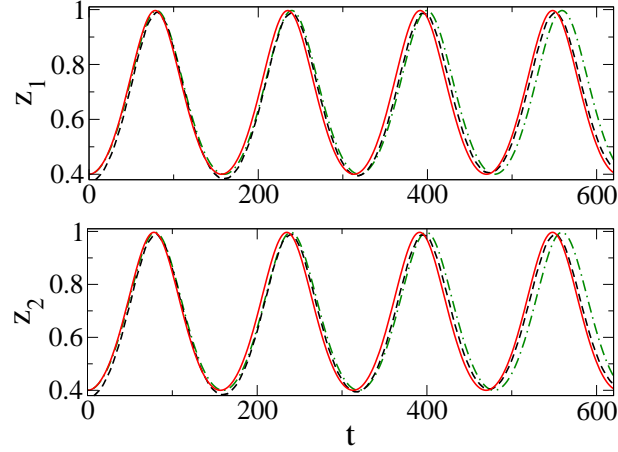


Figure 4. Fractional imbalance of the first and second bosonic vs. time. The dashed line represents data from integration of Eq. (8), the dot-dashed line represents solution of Eq. (21) with  $K_1 = K_2 = K = 0.0148$ , and the continuous line represents solution of Eq. (21) with the best-fit  $K$  equal to  $0.0151$ . Here is  $U_1 = U_2 = 0.1K$ ,  $U_{12} = 0.14K$ ,  $N_1 = N_2 = 100$ . We used the initial conditions  $z_i(0) = 0.4$  and  $\dot{z}_i(0) = 0$ . The units are as in Fig. 1 and in Fig. 2.

The condition to find  $U_{12}^{(II;cr)}$  is the Eq. (34), and we obtain that  $U_{12}^{(II;cr)}$  coincides with  $U_{12}^{(I;cr)}$ .

An interesting task, now, is to analyze the influence of the interaction between the two BECs on the temporal evolution of the fractional imbalances. We have fixed  $U_1$  and  $U_2$ , and analyzed  $z_1(t)$  and  $z_2(t)$  for different values of the inter-species interaction amplitude  $U_{12}$ . The greater is the absolute value of  $U_{12}$ , the greater is the deformation of the oscillations around  $\langle z_i(t) \rangle = 0$ , as shown in the two upper panels (from left to right) and in the first lower panel (from the left) of each  $z_i(t)$  represented in Fig. 3. Note that as long as the oscillations are harmonic (see the first panel of each  $z_i(t)$ ), the time evolution of the fractional imbalances may be described in terms of a carrier wave of frequency  $\omega_c$ , given by Eq. (26) with  $U_{12} = 0$ , modulated by a wave of frequency  $\omega_m$ . The frequency  $\omega_c$  is much greater than  $\omega_m$ . We found that there exists a value of the inter-species interaction amplitude for which the relative population in each trap oscillates around a non zero time averaged value,  $\langle z_i(t) \rangle \neq 0$ , which corresponds to the macroscopic quantum self-trapping (MQST) as discussed in [4] for a single component. To support this interpretation, we have studied the behavior of the density profiles of the two species as function of  $z$  and for different values of time. In particular, to find  $\langle \rho_i(z;t) \rangle$ , we have numerically solved the two coupled GPE (8) for those values of the interaction amplitudes for which the self-trapped is predicted to occur by the coupled pendula equations. We have summarized the results of this analysis in the last two panels of Fig. 3. Finally, it is interesting to observe that there is a good agreement between MQST predicted by the coupled pendula equations (21) and the one got by numerically solving the two 1D GPE (8). This comparison is displayed in Fig. 4, where we can observe oscillation around a non zero time averaged value of fractional imbalances. We

followed the same fitting procedure adopted in obtaining Fig. 2.

At this point, we observe that the question of the AJJ with two bosonic species could be addressed also from the experimental point of view. This could be done considering, for example, BECs binary mixtures of two bosonic isotopes of the same alkali atom [12]. The works referenced in [8] and [9] provide the ideal guide lines for this kind of experiments. By engineering a double well potential as suggested, for instance, by Gati et al. [9], the measured fractional imbalances  $z_i(t)$  could be compared with the ones obtained both by solving the Eq. (8) (see [8] and [9]) and the ODE system (21). It could be possible to measure, moreover, the inter-species s-wave scattering length  $a_{12}$  by using, to test the ideas, the frequency (26). The mixture could be prepared in such a way that both all the conditions  $z_1(0) = z_2(0)$ ,  $K_1 = K_2$ ,  $U_1 = U_2$ ,  $N_1 = N_2$  – see the discussion about the four classes (i)–(iv) of stationary points – are verified and to have small amplitude oscillations around the stationary point (i). Each  $z_i$  oscillates according to the law  $z_i(0) \cos(\omega^{(1)} t)$  (see Eq. (27)). Let us suppose to test both the characteristic quantities (in our case, they are  $\omega_i$ ,  $a_i$ ,  $z_0$ ) of the trapping potential – the group of Heidelberg displayed how this is possible for a given class of double well traps [8], [9] – and the intra-species s-wave scattering length  $a_i$ . Then, the functions  $\phi_i$  are known. Then, the Eqs. (12) provide the parameters  $K_i$  and  $U_i$ . The measure of the period of  $z_i(0) \cos(\omega^{(1)} t)$  leads to the corresponding frequency  $\omega^{(1)}$ , i.e. the left-hand side of Eq. (26). The solution of this equation gives the parameter  $U_{12}$ . By the mean of the second line of Eq. (12) one gets  $g_{12}$ , and, then  $a_{12}$ .

### 3. Conclusions

We have analyzed the atomic Josephson effect in presence of a binary mixture of BECs. We have written the Lagrangian of the system, from which we have derived a system of coupled differential equations which governs the dynamical behavior of the fractional imbalance and of the relative phase of each component. We have analyzed the stable points that preserve the symmetry, and we have obtained an analytical formula for the frequency oscillations around these equilibrium points. To this regard, one of the most interesting features is the possibility to know the inter-species s-wave scattering length from these frequencies. We have shown that in correspondence of precise values of the inter-species interaction amplitude, the relative populations oscillate around a non zero time averaged value. This behavior corresponds to MQST, a well-known phenomenon when only one component is taken into account. We have compared the predictions of GPE with the ones of the coupled pendula equations. We have performed this comparison in the case of total absence of interaction, in the case in which only the intra-species interaction is present, and in the case in which also the inter-species interaction is involved. We have found that, under certain conditions, the predictions of GPE agree with those ones of the coupled pendula equations. We have shown that, under certain hypothesis, it is possible to obtain analytical expressions for the inter-species interac-

tion amplitudes which signs the onset of the self-trapping. Finally, we have commented about the possibility to correlate our theoretical work with the experiments proceeding from the works of the group of Heidelberg, see [8] and [9].

This work has been partially supported by Fondazione CARIPARO through the Project 2006: "Guided solitons in matter waves and optical waves with normal and anomalous dispersion".

- [1] S.N.Bose, Z.Phys.26, 178 (1924); A.Einstein, Sitzungsber.K.Preuss.Akad.Wiss., Phys.Math.Kl.22, 261 (1924).
- [2] M.H.Anderson, M.R.Matthews, C.E.Wieeman, and E.A.Cornell, Science 269, 198 (1995); K.B.Davis, M.O.Mewes, M.R.Andrews, N.J.van Duten, D.S.Durfee, D.M.Kum, and W.Ketterle, Phys.Rev.Lett. 75, 3969 (1995); C.C.Bradley, C.A.Sackett, J.J.Tollett, and R.G.Hulet, *ibid.* 75, 1687 (1995).
- [3] A.J.Leggett and F.Sols, Found.Phys. 21, 353 (1991); I.Zapata, F.Sols, and A.J.Leggett, Phys.Rev.A 57, R28 (1998); A.J.Leggett, Rev.Mod.Phys. 73, 307 (2001).
- [4] A.Smerzi, S.Fantoni, S.Giovannazzi, and S.R.Shenoy, Phys.Rev.Lett. 79, 4950 (1997); S.Raghavan, A.Smerzi, S.Fantoni, and S.R.Shenoy, Phys.Rev.A 59, 620 (1999).
- [5] L.Salasnich, A.Parola, L.Reatto, J.Phys.B:At.Mol.Opt.Phys. 35, 3205-3216 (2002).
- [6] M.Salemo, Laser Physics, 4, 620-625 (2005).
- [7] A.Barone and G.Paterno, Physics and Applications of the Josephson effect (Wiley, New York, 1982); H.Otha, in *SQUID: Superconducting Quantum Devices and their Applications*, edited by H.D.Hahlbohm and H.Lubbig (de Gruyter, Berlin, 1977).
- [8] M.A.Ibez, R.Gati, J.Folling, S.Hunsmann, M.Cristiani, M.K.Oberthaler, Phys.Rev.Lett. 95, 010402 (2005).
- [9] R.Gati and M.K.Oberthaler, J.Phys.B:At.Mol.Opt.Phys. 40, 10, R61-R89 (2007).
- [10] C.J.Milburn, J.Corney, E.M.Wright, and D.F.Walls, Phys.Rev.A 55, 4318 (1997).
- [11] G.Thalhammer, G.Barontini, L.De Sarb, J.Catani, F.Minardi, and M.Inguscio, Phys.Rev.Lett. 100, 210402 (2008).
- [12] S.B.Papp and C.E.Wieeman, Phys.Rev.Lett. 97, 180404 (2006).
- [13] N.A.Kostov, V.Z.Enolskii, V.S.Gerdjikov, V.V.Konotop, and M.Salemo, Phys.Rev.E 70, 056617 (2004); K.Kasamatsu and M.Tsubota, Phys.Rev.A 74, 013617 (2006).
- [14] P.G.Kevrekidis, H.E.Nistazakis, D.J.Frantzeskakis, B.A.Malomed, and R.Carretero-Gonzalez, Eur.Phys.J.D 28, 181 (2004).
- [15] E.A.Ostrovskaya and Yu.S.Kivshar, Phys.Rev.Lett. 92, 180405 (2004).
- [16] H.A.Cruz, V.A.Brazhnyi, I.V.V.Konotop, G.L.Almov, M.Salemo, Phys.Rev.A 76, 013603 (2007).
- [17] A.Gubeskys, B.A.Malomed, and I.M.Merhasin, Phys.Rev.A 73, 023607 (2006).
- [18] F.Kh.Abdullaev, A.Gamali, M.Salemo, L.Tomio, Phys.Rev.A 77, 023615 (2008).
- [19] X.Xu, L.Lu, Y.Li, Phys.Rev.A 78, 043609 (2008).
- [20] I.I.Satija, P.Naudus, R.Balakrishnan, J.Heward, M.Edwards, C.W.Clark, Phys.Rev.A 79, 033616 (2009).
- [21] A.Simoni, M.Zaccanti, C.D'Errico, M.Fattori, G.Roati, M.Inguscio, and G.Modugno, Phys.Rev.A 77, 052705 (2008).
- [22] L.Salasnich and B.A.Malomed, Phys.Rev.A 74, 053610 (2006).
- [23] L.Landau and L.Lifshitz, Course in Theoretical Physics, Vol. 3, Quantum Mechanics: Non-Relativistic Theory, (Pergamon, New York, 1959).